IAC-22-A3.3B.x69999

Envelope, Propulsion and Navigation for a Martian Exploration Airship

Michael W. Biselx[a], Florentin Fellay[b], Vincent J. Roggli[c]

[a] *Master student at Ecole Polytechnique Fédérale de Lausanne, Route Cantonale, 1015 Lausanne, Vaud, Switzerland, michael.biselx@epfl.ch*
[b] *Master student at Ecole Polytechnique Fédérale de Lausanne, Route Cantonale, 1015 Lausanne, Vaud, Switzerland f_fellay@hotmail.ch*
[c] *Master student at Ecole Polytechnique Fédérale de Lausanne, Route Cantonale, 1015 Lausanne, Vaud, Switzerland, vincent.roggli@epfl.ch*

Abstract

Current Mars exploration mainly falls into two categories: global survey from orbit, or localized ground-level studies using rovers or landers. Mid-level regional studies would require an exploration vehicle capable of covering long distances. This could be fulfilled by an airship with significant flight autonomy, able to gather scientific data on large, currently unreachable areas of the Martian surface. The possible use of such an airship to explore low-altitude, rugged areas such as the steeper slopes of Valles Marineris was assessed in a preliminary feasibility study presented at GLEX 2021. The presented airship consisted of a hydrogen-filled envelope with a diameter of around 45 meters, and would be capable of carrying a hyperspectral camera of 10 kg.

This paper follows up on the aforementioned feasibility study by investigating the enabling technologies for such a mission, with a particular focus on envelope design, propulsion system choice and navigation / communication strategies.

The low-density, cold Martian atmosphere and its strong winds pose considerable challenges for the design of a lighter-than-air platform. In this paper, we explore these environmental challenges on the basis of the Mars Climate Database. First, the daily thermodynamic cycles of the lifting gas are simulated using a convective-radiative heat transfer model of the airship. The constraints imposed on the envelope geometry and materials by these cycles are then discussed and a case is made for the use of a ballast inner balloon for both lifting gas pressure and vertical control. Next, horizontal control is investigated in a trade-off study of different types of propulsion technologies. A preliminary design of the propeller propulsion system is established using blade element momentum theory and computational fluid dynamics. Using the power requirements for the propulsion system, a power budget for the airship's main subsystems is set up and used to dimension its solar cell array and on-board batteries. Then, the governing equations of the motion dynamics are used to create a numerical simulation, and some recommendations for the navigation and communications equipment are made. Finally, from a systems engineering perspective, a refined mass budget for the 900 kg airship is presented, as well as a preliminary concept of operations.

The results obtained show that the proposed Martian airship is not only feasible, but even a promising platform to bridge the gap between top-down global surveying and localized exploration.

Keywords — Airship, Mars, Exploration, Feasibility, Valles Marineris

Nomenclature

Acronyms

BEM	Blade Element and Momentum
C&DH	Command and Data Handling
CONOPS	Concept of Operations
COTS	Commercial Off-The-Shelf
DRM	Design Reference Mission
EPS	Electrical Power System
FSW	Flight Software
GNC	Guidance, Navigation and Control
IMU	Inertial Measurement Unit
LRN	Low Reynolds Number
MPC	Model Predictive Control
MRN	Mars Relay Network
MRO	Mars Reconnaissance Orbiter
OBC	On-Board Computer
SLAM	Simultaneous Localisation And Mapping
TGO	Trace-Gas Orbiter
TT&C	Tracking, Telemetry and Control
UHF	Ultra-High Frequency
VIS/NIR	Visual/Near-InfraRed

Physical Constants

g	Mars Gravity ($3.721 \mathrm{ms}^{-2}$)

Symbols

α	Angle of attack
η	Efficiency
Ma	Mach number
Re	Reynolds number
Π	Superpressure
Θ	Supertemperature
a	Speed of sound
c	Chord length
c_d	Section Drag Coefficient
c_l	Section Lift Coefficient
d	Drag per unit span
J	Propeller advance ratio
l	Lift per unit span
L_S	Solar Longitude
n	Propeller rotation rate
P	Power
Q	Torque
T	Thrust
v	Airspeed

1 Introduction

1.1 Study Background

Current Martian planetary exploration is mainly achieved through orbiters, landers and rovers. Each of these methods gives insight into the active processes of a planet at different scales :

Orbiters have a global bird's-eye view of the studied world, permitting the investigation of global-scale events and processes — on the other hand, they are not able to linger and observe events happening on the surface in great detail.

Landers allow scientists to extensively study a single point on the planetary surface over a longer term, observing seasonal variations and rare events — in consequence, however, they are stuck in place, and can only sample a single location.

Rovers, in turn, are able to travel across the planet's surface, exploring the terrain and visiting multiple locations, returning large amounts of valuable data. Yet despite engineers' best efforts, there are locations that are unattainable to wheeled vehicles, such as steep slopes or broken terrain.

To remedy this last point, NASA came up with a new concept, the Mars helicopter. Its demonstrator *Ingenuity* [1] proved the feasibility of Martian atmospheric flights. However, due to their heavier-than-air nature, the flights of such helicopters are relatively short. Moreover, the vehicle requires safe spots for landing and recharging. The same goes for most other Martian powered flight projects.

Our team proposes a flying platform for scientific instruments which would not be subject to such restrictions: an *airship*. Indeed, a lighter-than-air dirigible aircraft would be able to safely investigate the rugged terrain of one of Mars' most inaccessible features, *Valles Marineris*, and help find answers to some of the essential scientific questions surrounding the formation of this 10 km deep and 4000 km long rift in the Martian surface.

Figure 1: Artist's impression of the proposed Martian Airship

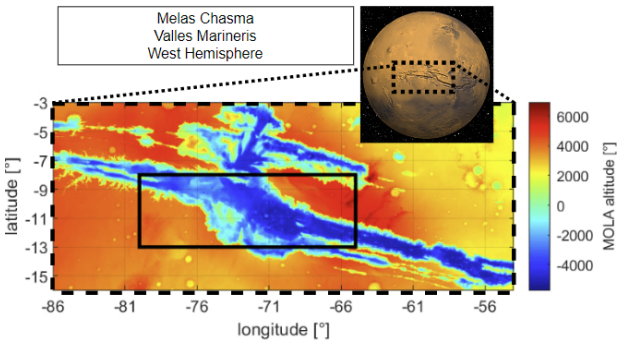

Figure 2: Melas Chasma in Valles Marineris is the exploration site selected in the DRM.

Table 1: Reference parameters for the DRM

Name	Symbol	Value
reference latitude	ϕ	10° S
reference longitude	λ	70° W
reference altitude	h	-2500 m
reference solar longitude	L_S	45°

Table 2: Airship parameters according to the DRM

Name	Symbol	Value
Balloon nominal diameter	D_b	46 m
Nominal airspeed	v	10 m/s
Airship nominal mass	M	900 kg
Airship payload mass	-	10 kg

1.2 Study History

The use of lighter-than-air aircraft is not unheard-of in planetary exploration. In 1984-85, the Soviet Union's *Vega* missions to Venus included a pair of weather balloons whose purpose was to investigate the planet's upper atmosphere. In the late 1980's-90's, a number of space agencies investigated and developed concepts for free-floating Martian exploration balloons, notably NASA's *Mars Aerobot Balloon Study* (MABS) [2], and CNES's *Montgolfière Infra-Rouge* (MIR) [3], among others. In recent years, there has been a reawakening of interest in powered aerostatic flight on Earth, which has been boosted by new materials and control techniques.

The present study began in September 2020, as a semester project for the EPFL Space Technologies Minor, in collaboration with the WoMars association, and the Mars Society Switzerland. The initial goal was a general feasibility study of a Martian airship, as well as the establishment of a Design Reference Mission (DRM). This work was presented at GLEX 2021 [4] by Tonasso et al. In September 2021, a second round of feasibility studies were carried out, intended to refine models and hypotheses used in the first study, and initiate the first design iterations of selected subsystems.

2 Airship system

2.1 Mission

The Martian airship DRM established in the first year of the study has since been refined and modified. It is briefly summarized in the following paragraphs.

The proposed DRM would send an airship equipped with a VIS/NIR hyperspectral camera to *Melas Chasma* in *Valles Marineris*, see Figure 2, in order to analyze sediment composition and weathering patterns up close.

The choice of *Valles Marineris* as destination is due both to technical and scientific reasons — scientifically, it is a location with interesting resources (such as possible water-ice deposits [5]), atmospheric phenomena (such as cloud and fog formation [6, 7]), and weathering processes (such as recurring slope lineae [8]). From a technical/engineering perspective, the extremely thin Martian atmosphere makes it difficult for aerostats to achieve lift anywhere but at the lowest altitudes. With depths ranging from -1000 m to -5000 m altitude[1], *Valles Marineris* is a relatively good candidate for experimentation with this sort of craft. Additionally, due to its proximity to the equator, *Valles Marineris* enjoys a relatively clement climate year-round, as well as a good potential for solar power generation.

The main change to the DRM we propose in this paper is the season of activity. In [4], Tonasso et al. proposed that the mission take place at a solar longitude of $L_S = 270°$. For reasons which shall be argued further on in this paper (see subsubsection 3.3.1), we would instead suggest $L_S = 45°$ as a candidate season.

2.2 Airship System Overview

The system breakdown structure of the proposed airship can be found in Figure 3. The corresponding mass budget with contingencies is given as well, see Figure 5. The whole airship is expected to weigh between 750 kg and 950 kg, though there is still a fairly large margin of uncertainty on many of the subsystems.

In the following paragraphs, we shall briefly discuss the subsystems which are of particular importance for this paper.

2.2.1 Electrical Power System

The Electrical Power System is responsible for power generation, storage and distribution aboard the arship.

[1] Altitudes are based on the measurements made by the Mars Orbiter Lazer Altimeter (MOLA) mission

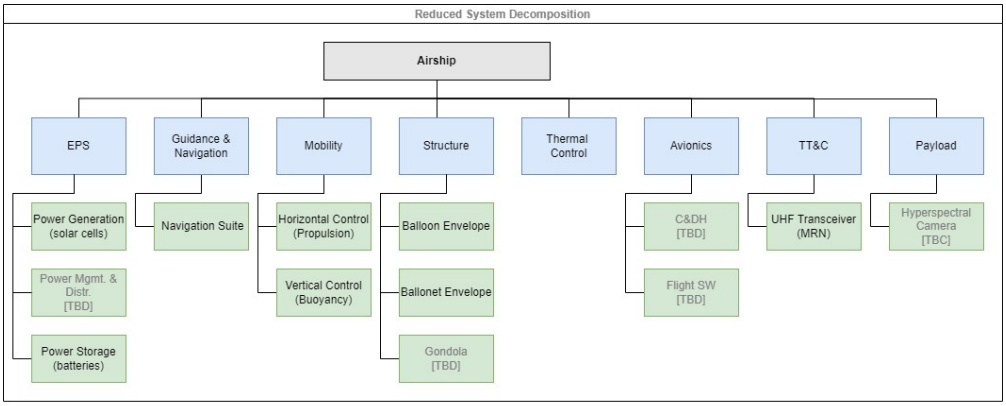

Figure 3: Martian airship system breakdown structure

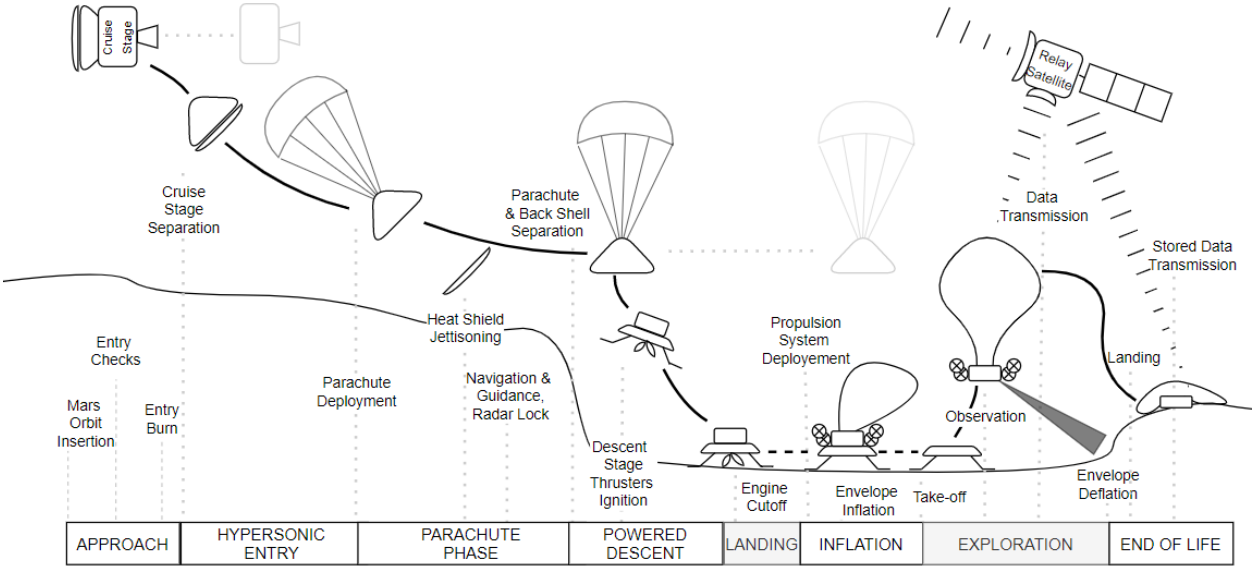

Figure 4: Proposed concept of operations (ConOps)

2.2.2 Guidance and Navigation

The Guidance and Navigation subsystem is responsible for determining the airship's position and attitude. For the localization, a suite of different sensors is used (described in subsubsection 3.5.2).

2.2.3 Mobility

The airship has two methods for mobility : firstly, control of the amount of lift generated is achieved using an inner balloon, located inside the airship's lifting body, for ballast, and thus affording the airship some vertical control. Secondly, the propeller-based propulsion system gives the airship mobility in the horizontal directions. The propulsion system is discussed in greater depth in subsection 3.2.

2.2.4 Structure

The Structure subsystem interfaces all the functional parts of the airship. It consists of the envelopes of the lifting body and the inner balloon (which will be presented in subsection 3.1), and the solid structure of the gondola (which houses the various pumps, valves and tanks, the scientific payload, the thermally controlled electronics and the batteries).

2.2.5 Thermal Control

The Thermal Control subsystem will be particularly critical for the propulsion system and the batteries, as these will generate a lot of heat. As the thin Martian atmosphere is a very poor heat conductor, care will need to be taken to make sure that none of these critical systems overheat. Additionally, heat dissipation will require radiators,

System/Subsystem	Units	Unit Mass [kg]	Contingency [%]	Total Mass [kg]
Airship				
EPS				**270.3**
Power Generation				131.2
Solar cells		*93.7*	*40%*	*131.2*
Power Mgmt. & Distr.				2.8
Power Bus		*2.0*	*40%*	*2.8*
Power Storage				136.4
Batteries		*113.6*	*20%*	*136.4*
Guidance & Navigation				**13.6**
Navigation Suite		9.7	40%	13.6
NavCams	*5*	*1.5*		
Ranging Radar	*4*	*0.5*		
IMU	*2*	*0.1*		
Mobility				**76.1**
Horizontal Control				40.1
Electrical Engines	*4*	*0.6*	*10%*	*2.6*
Transmission	*4*	*0.4*	*40%*	*2.2*
Propellers	*8*	*4.0*	*10%*	*35.2*
Vertical Control				36.0
Lifting Gas		*30.0*	*20%*	*36.0*
Valves				
Pumps				
Hydrogen Tank				
Structure				**534.5**
Balloon Envelope				408.0
Gores		*340.0*	*20%*	*408.0*
Tendons				
Ballonnet Envelope		33.2	40%	46.5
Propulsion Framework		10.0	100%	20.0
Gondola		30.0	100%	60.0
Thermal Control			**100%**	
Avionics				**18.2**
C&DH		13.0	40%	18.2
OBC	*2*	*3.0*		
Data Storage				
Harness		*10.0*		
Flight SW				0.0
Visual SLAM				
Control Software				
Data Compression				
TT&C		**3.4**	**40%**	**4.8**
UHF Transciver		3.0		
UHF Antennae		0.4		
Payload		**10.0**	**40%**	**14.0**
Hyperspectral Camera				
Stabilization & Pointing				
TOTAL				**931.4**

Figure 5: Provisional mass budget of the airship system

which will have an important effect on the mass and power budgets.

The thermal control for the airship not part of this report, and still remains to be investigated.

2.2.6 Payload

The Payload is the airship's means of accomplishing its scientific objective. It is expected to be a VIS/NIR hyperspectral camera, which will require active stabilization. The mass budget reserves 10 kg for this instrument.

2.3 Airship Mission ConOps

The following Concept of Operations (ConOps) is considered for the mission (see Figure 4) :

The mission is launched from Earth at such a date that the arrival time corresponds roughly to the correct Martian season (about L_S=45°).

After a successful Earth-Mars transfer, the spacecraft is inserted on a Mars parking orbit. At this stage, the airship is folded and mounted on a descent module. Both are protected by an aeroshell. Once all entry checks are complete (functional tests, weather conditions on landing site, etc.), the cruise stage performs a final entry burn to set the entry spacecraft on a proper trajectory. This approach phase is concluded by the cruise stage separation.

The airship is protected by a heat shield during the hypersonic entry. It is further decelerated by a parachute. At the end of this phase, the heat shield is jettisoned and the navigation and guidance systems are activated.

For the last meters of descent, the folded airship is separated from the back shell and is safely landed in *Melas Chasma* by the descent module.

Once on the Martian ground, the airship deployment procedure can start. The envelope is inflated with hydrogen from the descent module's tanks, the solar arrays start to produce power, and the propulsion system is deployed. Once all systems are ready, the airship is released from the descent module and can start its exploration activities, sending back highly compressed versions of the data gathered by onboard sensors through the Mars Relay Network's relay satellites.

The end of the flight phase of the mission is nominally marked by the airship no longer being able to generate sufficient lift to stay aloft, due to the loss of hydrogen by diffusion through the envelope. The airship lands gently on the Martian ground. At this point, the envelope is progressively deflated, in a way that the solar arrays are still exposed to solar radiation. The transmission of the cached raw data is initiated, and periodic local environmental observations are performed and reported.

3 Subsystems Preliminary Concept

This chapter is dedicated to the description of five fundamental parts of the airship: envelope, propulsion, power, data handling and navigation subsystems. Early design considerations are presented here, along with the methodologies used to estimate the sizing of these various subsystems. Ultimately, these findings were used in the global mass budget to demonstrate the feasibility of aerostatic flight of the airship.

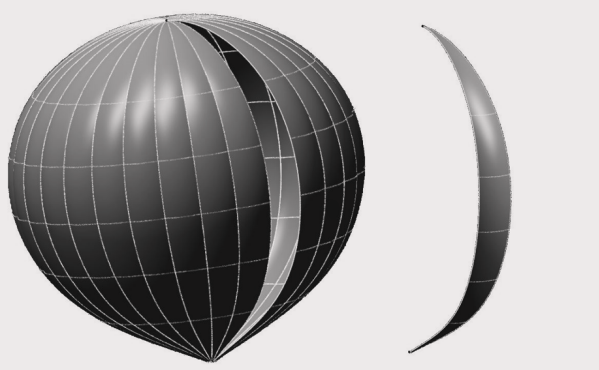

Figure 6: Pumpkin-shaped envelope, made of individual gores (right)

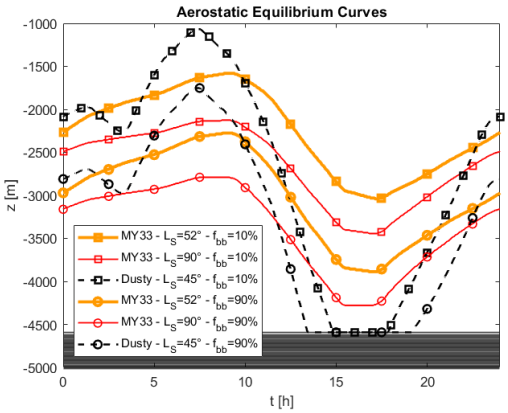

Figure 7: Equilibrium trajectories during a sol for different flight reference conditions, starting from midnight local time. f_{bb} is the inflation ratio of inner balloon filled with martian air.

3.1 Envelope Design

The main function of the envelope is to contain the lifting gas, and thus provide lift for the airship. It is made of a triple-layer composite material, the thickness of which is determined by the maximum pressure inside the balloon. The envelope also contains the inner ballast balloon, and the upper surface is used for power generation.

3.1.1 Sizing

According to the previous study by Tonasso et al., an envelope of approximately 46 m diameter would be required to generate sufficient lift for this mission. Given the need for a large capacity, long duration balloon, a design based on a hydrogen-filled superpressure balloon was chosen. It means that the internal hydrogen pressure is higher than atmospheric pressure.

Since the atmosphere on Mars is very thin and the aerodynamic effects quite low, a near-spherical shape was chosen : the pumpkin shape. The pumpkin shape is made up of gores out of a composite film connected by tendons: These reduce the stress in the film [9], requiring less material (and therefore less mass).

Hydrogen is used as a lifting gas. While it is optimal in terms of buoyancy, it poses some challenges regarding its containment due to its small atomic size and tendency to diffuse through most materials. Low permeability is thus a required characteristic for the outer envelope and inner balloon materials.

An inner ballast balloon, sometimes called ballonet, is necessary for vertical motion control. Pumping ambient air in and out of this balloon located inside the main envelope changes the weight of the airship, and therefore its altitude. A 23 m diameter inner balloon provides vertical control over a range of about 800 m.

3.1.2 Aerostatic Equilibrium

The atmosphere of Mars is characterised by large daily variations in density. Understanding the influence these variations will have on the airship's movement is critical.

Using the Mars Climate Database (MCD) [10], the static vertical equilibrium altitude was calculated for the airship at every hour of the sol, for several seasons (see Figure 7). During the cool early-morning hours, the airship produces a lot of lift in the dense, cold atmosphere, and thus follows a generally ascendant trajectory. Once the day advances and the air heats up, the atmosphere becomes thinner and the airship begins to sink again. We suggest to exploit these daily fluctuations of more than a kilometer altitude and allow the airship to make this natural sweep. This strategy permits to observe several rock strata of Valles Marineris without any effort.

Using the calculated aerostatic equilibrium trajectories, it was determined that the best season for deployment lies between $L_S = 0°$ and $L_S = 90°$. Conversely, the worst possible deployment scenario is that of a dust-storm, as the resulting higher temperatures decrease the atmospheric density and reduce the airship's lift below the minimum requirement.

3.1.3 Constraints and Limitations

The lifting gas inside the envelope must be maintained at a higher pressure than the surrounding atmosphere in order to keep the balloon from collapsing under its own weight. This will dictate both the minimum required material thickness to contain the pressure, as well as the minimum amount of hydrogen to be taken along.

The superpressure ratio f_Π is defined as the ratio between the internal hydrogen pressure and the atmospheric pressure. These can be calculated using the MCD

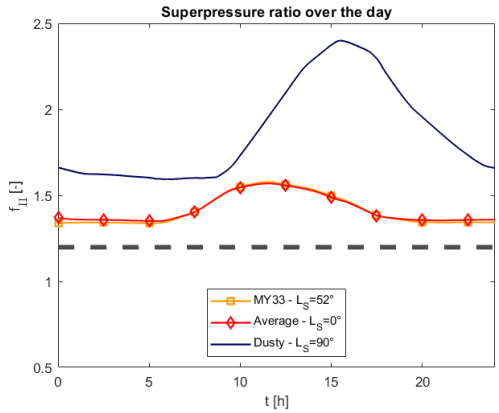

Figure 8: Evolution of internal pressure over a typical sol for an initial hydrogen mass of 30 kg

and a thermal model of the airship. The evolution of this parameter over a typical day is illustrated in Figure 8, where the horizontal dashed line represents the inflation limit at which the envelope collapses under its own weight. This to was calculated to be about 1.2 times the surrounding atmospheric pressure. Additionally, the maximum pressure determines the thickness of the composite envelope from which follows the mass. It should be noted that a dusty atmosphere scenario would lead to much thicker envelope requirements, due to the warmer atmosphere heating the lifting gas in the envelope. This underscores the importance of avoiding dust-storm scenarios at all costs. Otherwise, the pressure inside the envelope is not greatly subjected to seasonal variations as shown with the overlay of orange and red curves.

The three layers of the envelope material each have a specific function: The radiative properties, the mechanical resistance and the low permeability are the relevant parameters, as already noted by Tonasso et al. [4]. In particular, a fibrous layer is suggested to increase mechanical resistance.

The last degree of freedom in the design concerns the hydrogen quantity to be embarked at the beginning of the mission. It will determine the duration of the flight phase of the airship's mission. There are two conceivable scenarios to contain hydrogen:

- An additional H2 tank aboard the gondola that can refill the balloon during the mission. The periodic injection of hydrogen shall ensure that the superpressure ratio stays above the inflation limit.

- No additional H2 tank and thicker envelope to withstand higher pressure difference.

Table 3: Mean and extreme values of drag force and mechanical drag power.

L_S		0°	90°	180°	270°
Mean Drag	[N]	211.1	97.8	227.3	369.4
Max Drag	[N]	418.9	239.1	641.9	1013.2
Mean Power	[kW]	1.57	0.5	2.16	4.14
Max Power	[kW]	4.17	1.8	7.91	15.69
Daily Budget	[kWh]	39.2	12.6	N/A*	103.4
Night Budget	[kWh]	30.1	3.13	N/A*	88.0

*Missing values (N/A) indicate that the airship is grounded due to insufficient buoyancy.

3.2 Propulsion

This section is dedicated to the elaboration of a propulsion system responsible for the horizontal control of the airship, an indispensable feature for a safe exploration of the deep *Valles Marineris* canyon system. In the following sections, we shall investigate the challenges offered by the Martian environment on a propeller-driven airship and present the methods used for early design considerations.

In a first phase, a review of available state-of-the-art atmospheric propulsion systems was conducted, based on Colozza et al. [11]. It was concluded that the most suitable propulsion system for a Martian airship would be battery-powered propellers. This provides greater endurance, minimized mass and reduced costs compared to alternatives.

3.2.1 Propulsive power requirements

In a second phase, the propulsion requirements were established based on the Martian environment and atmosphere. The sizing of the propulsion system must be such that the airship can cope with the everyday winds and avoid collisions with the canyon walls. The propulsion system must be able to compensate the force of the wind drag at any time of the day, and have the endurance to do so for the duration of the day (and night). This gives us the minimum power and energy requirements.

The Mars Climate Database (MCD) [10] was again used to find the wind speed along the aerostatic equilibrium trajectories presented in Figure 7. This lets us calculate the drag force and associated power caused by the winds using drag coefficients recommended by the Scientific Ballooning Handbook [12], under the assumption of a spherical envelope. The result is an instantaneous value of drag for each time of day (see Figure 9).

This is then accumulated over the sol to obtain the required daily and night budget of propulsive energy, see Table 3. Note that these quantities are all expressed in terms of propulsive power P_{prop}, which is obtained by the propeller from the mechanical power of the engine P_{eng}. This conversion is associated to a certain efficiency

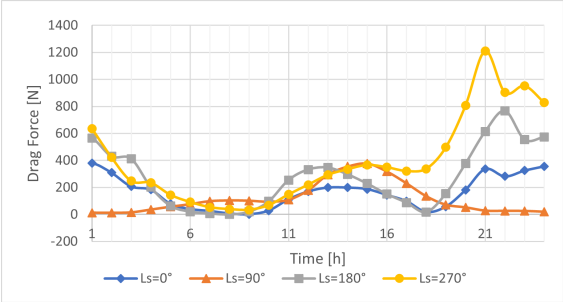

Figure 9: Drag force at aerostatic equilibrium altitude over the course of a sol.

$\eta_{prop} = \frac{P_{prop}}{P_{eng}}$, which is a critical parameter as it drives engine and battery selection. Special effort has to be made to optimize it. This is the subject of the following sections.

3.2.2 Propeller design constraints

The very thin atmospheric density ρ on Mars limits the drag acting on the airship. However, it also poses a serious challenge to the propeller design. The chord-based Reynolds number $Re = \frac{\rho v c}{\mu}$, defined as a function of the flow velocity v, airfoil chord c and dynamic viscosity μ, is reduced to $Re \sim 20'000 - 60'000$, two orders of magnitude lower than in Earth low atmospheric conditions. This leads to complicated, not fully understood flows. Common airfoils show degraded performance in such circumstances, and are likely to stall at relatively low angles of attack.

Another challenge comes from the composition of the Martian atmosphere, consisting of 95% of CO_2. This has a large impact on the local speed of sound, which has been confirmed by Maurice et al. to be only around $a_{\mathcal{O}^{\nearrow}}$=240 m/s [13]. This leads to larger Mach numbers $Ma = \frac{v}{a}$ at the propeller tips. Yet, sonic conditions must be avoided at all costs, since it will ruin propeller performance, and even damage the blades. This limits the size and speed of the propellers.

The last major design issue which must be addressed is the advance ratio of the propeller, defined as $J = \frac{v}{nD}$, with n the rotation speed of the propeller in [rps] and D the propeller diameter. By design, the airship's airspeed should not exceed 10 m/s, which gives a very low advance ratio. We will see later, in paragraph 3.2.4.1, that propellers have a very low efficiency in such regimes.

3.2.3 Airfoil Selection

A propeller blade is nothing else than a spinning wing. The design of its section, or airfoil, is thus very similar to that of a wing, except that the lift of the blade is used to propel the airship, and its drag is directly opposed to the engine torque. Efficiency is maximized by optimizing the airfoil lift to drag ratio c_l/c_d. Therefore, the angle and twist of a propeller blade must be designed so that it operates at the optimal angle of attack α on its whole span.

Lift and drag coefficients of classical airfoils are easily found in the literature for various Reynolds numbers as a function of α in the form of polar plots. Unfortunately, the performance of classical airfoils at low Reynolds numbers (LRN) is known to be poor, with stalls observed even at relatively low angles of attack. An abundant literature exists on this topic [14, 15, 16, 17, 18], as it has become a genuine problem for wind turbines, unmanned aerial vehicles (UAV), micro air vehicles (MAV) and Mars helicopters. All these devices operate at LRN, albeit for different reasons (density, inflow velocity or size).

Wind tunnel testing as well as computed fluid dynamics show that thin and cambered airfoil behave better in such conditions. The Mach number has a limited influence so long as subsonic conditions are preserved. Note that the airfoil shape, and in particular its thickness, is constrained by the structural stress inherent to the propeller rotation and fluid-structure interactions.

3.2.4 Propeller Design

It is interesting as well to investigate how the whole propeller reacts to the characteristics of the Martian atmosphere. Some simple models are very useful for early design calculations.

3.2.4.1 Froude momentum theory

The Froude ideal model is used first [19]. The idea is to consider the propeller as a virtual actuator disc providing a pressure jump. All aerodynamic and compressibility effects are ignored. A simple momentum balance permits to extract an ideal propeller efficiency. This provides an upper bound for the actual efficiency.

The ideal efficiency of a propeller providing 50 N thrust is mapped against propeller diameter and free-stream velocity in Figure 10. The dashed line corresponds to the expected airship airspeed. The graph shows rather disappointing values, mostly due to the very low density of the Martian atmosphere. The low airship airspeed does not help either. It is also deduced that larger propeller have better efficiencies. On the other hand, lowering the propeller thrust improves its efficiency.

A possible strategy for reducing the negative effect of the low advance ratio consists of having two propellers in a push-pull configuration. The second propeller benefits from the slip-stream velocity of the first one to increase its own advance ratio. This would increase the performance of the second propeller, while only slightly perturbing the first one. This configuration is of great interest for airships, whose velocities are very low, but would need further development to make sure this is indeed favorable.

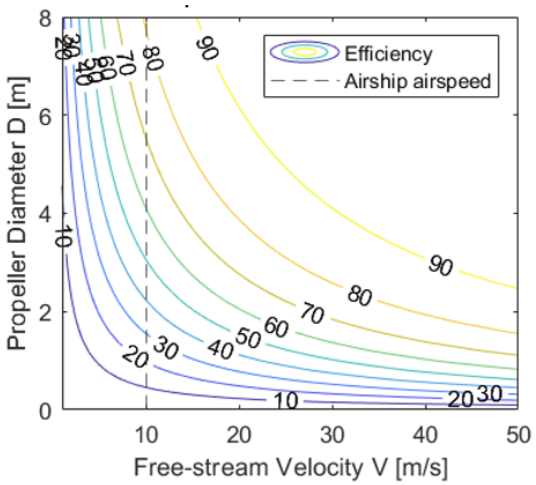

Figure 10: Ideal efficiency η_i [%] of a propeller with 50 N thrust

3.2.4.2 Blade Element Momentum method

For better predictions, the momentum equations are coupled to the blade element method (BEM). As the name suggests, the blade is discretised in a certain number of elements whose aerodynamic and geometric properties are known and used as input. This permits to evaluate the efficiency, thrust and torque of the propeller given its characteristics, such as blade number, diameter, pitch, etc. The limitation of this theory is that it does not include 3D effects or blade interactions. According to Auld and Srinivas [19], the efficiency obtained will be 5-10% higher than the real efficiency. Nonetheless, this is a great tool for optimizing the number of blades and pitch settings.

The BEM consists in solving equilibrium equations at each blade element to obtain the elementary thrust δT_i and torque δQ_i. They are summed up to obtain the total thrust T and torque Q, from which the input mechanical power P_{mec} is deduced. Finally, the propeller efficiency is usually given as a function of the propeller advance ratio, defined as $J = \frac{V}{nD}$.

A MATLAB script was written to iteratively solve the non-linear system of 6 equations obtained with BEM. The code interacts with XFOIL[2] [20] to retrieve the aerodynamic characteristics of the blade element profile. Figure 11 shows the calculated performance of a two-bladed, 2 m diameter airscrew operating at 1455 RPM. In these conditions, the blade tip Mach number is 0.8. The three graphs indicate the propeller efficiency, power, thrust and torque. The dashed line in the graphs represents the 10 m/s nominal airspeed of the airship. At this speed, the propeller efficiency is barely 30% (consistently below the ideal efficiency shown in Figure 10). It provides a thrust or 40 N for an input power of about 1250 W. Five of these propellers would be needed to power the airship.

The script is then used to optimise each propeller parameter separately :

- RPM: The higher the propellers RPM, the higher the thrust. Moreover, higher RPM give higher Re and better behaviour of the airfoil. However, the Mach number at the blade tip must be limited to a maximum of 0.8 in order to avoid losses and destructive supersonic shock-waves.

- Pitch: Another important parameter is the blade angle, also called geometric pitch. The propeller pitch is usually constant along the blade in order to have a constant and optimal angle of attack (the outer part having a larger angular velocity for the same inflow velocity), though a complete optimisation of the blade angle would also require an additional twist. In general, increasing the pitch shifts the efficiency curve to the right (towards larger velocities) and also increases the maximal thrust. It should be ensured that the pitch and twist are set properly. The JAVAPROP software does a decent job for that purpose. Variable pitch propellers can be discarded, as they require heavy mechanisms for little benefit given the small airspeed range of the airship.

- Number of blades: Although a higher thrust comes from an increased blade number, it also reduces its global efficiency. Propellers with a large number of blades are normally reserved to large power plants. Thus, for a lightweight electrical motor, the optimal choice is probably based on multiple two-bladed propellers.

- Number of propellers: Some of the possible configurations meeting the propulsion requirements are sets of 4 $\times$ 3 m, 6 $\times$ 2 m or 8 $\times$ 1.5 m propellers.

The previous development was focused on propeller aerodynamic performance and loads, with the aim of maximizing the propeller efficiency. Now, a propeller is experiencing severe mechanical loads that also have to be accounted in the design in order to also minimize its weight. Recent developments in material science allow the use of carbon fiber composite propellers, which are unbeatable in terms of weight. However, heavy reinforcements are required on large, fast spinning propellers. The current design philosophy for eVTOL and UAV's tends towards having a large number of small propellers.

3.2.5 Proposition of a propulsion system

As a conclusion to this part, we propose a propulsion system powered by a battery stack charged by solar cells.

[2] XFOIL is an interactive program designed to analyse subsonic flows around an airfoil with the panel method.

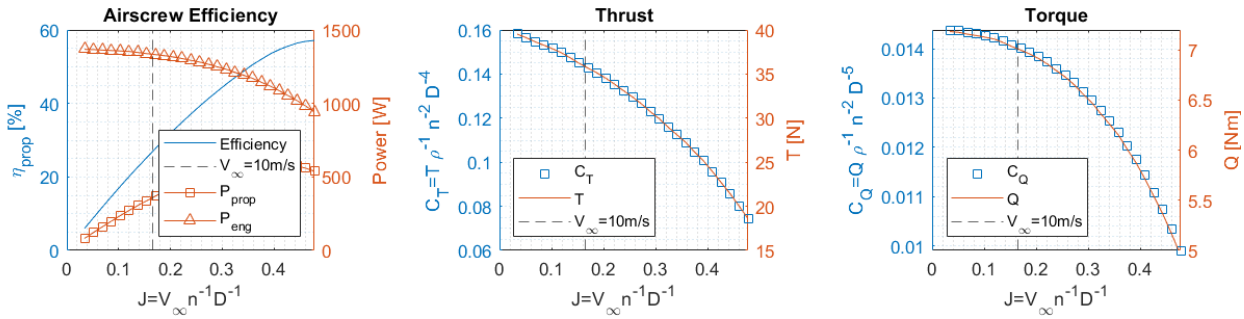

Figure 11: Performance of a two-bladed, 2 m diameter propeller at 1800 rpm ($\mathrm{Ma}_{tip} = 0.8$)

Thrust is generated by four pairs of counter-rotating propellers, each powered by a brushless DC engine : The large number of propellers permits a good load distribution and their counter-rotating configuration enhances the compactness and efficiency of the system.

The propellers sets are mounted on the gondola at the end of deployable arms, which are kept stowed for the trip to Mars. The positioning of the propellers around the gondola is such that it allows some attitude control for the airship. The weight of the whole propulsion system is estimated between 58 kg and 74 kg, with contingencies.

3.3 Electrical Power System

Several options were considered for powering the airship. With current and near future technologies, solar power generation with battery storage was considered optimal. The idea is to take advantage of the large surface of the envelope by covering the top with solar cells. In addition, power storage is needed to compensate the lack of power production during the night.

3.3.1 Power Requirements

The greatest part of the power consumption is attributed to the propulsion system, which must constantly compensate the Martian winds. This consumption is deduced from the results of propulsive power, see subsubsection 3.2.1, considering an overall efficiency of 22% for the propulsion system. All other subsystems will have comparatively lower power requirements. They shall be evaluated in a later phase of the project.

3.3.2 Power Generation

Power generation for the airship shall be accomplished by lightweight and flexible thin-film photovoltaic cells on the upper surface of the envelope.

To estimate the surface of cells required, we consider that the generated power must be sufficient to both cover the peak instantaneous power requirements of the propulsion system, and to recharge the batteries over the course of the 10 daylight hours of a sol. Thus, considering a mean solar radiance of 240 W/m^2 during daylight hours, and an efficiency of 15% for the thin-film solar cells, we can estimate that about 260 m^2 of solar cells will be needed (covering about 4% of the envelope surface). Assuming a mass per area of 0.35 kg/m^2, this works out to a total mass of around 94 kg for power generation.

There is definitely enough space to generate sufficient power. What is more challenging is the implementation of the solar cells on the envelope. Indeed, the envelope is folded until its deployment on the Martian surface. Thus, an additional requirement arises for the solar cells: foldability. This is a particularly difficult requirement to satisfy. Either large improvements will need to be made in flexible solar cell technologies, or a deployable system must be designed, which comes with its own challenges.

3.3.3 Power Storage

Due to the use of solar panels for power generation (see subsubsection 3.3.2), which provide a non-constant source of power, there is need to generate excess power when sunlight is available in order to store it for use during the night-time.

Based on the previously determined mechanical drag power over the course of a day, it is possible to estimate the energy requirements for 14 non-sunlight hours (see Table 3). The optimal season for the mission is therefore clearly $L_S = 90°$, as it has the lowest power demands — especially during night-time, when solar energy is not available.

This means that the airship would require sufficient batteries to store at least enough electrical energy to produce the predicted 0.5 kW of mean *mechanical* power at night.

Considering again the expected low aerodynamic efficiency of the propulsion system (22%, see paragraph 3.2.4.1) and the admissible 80% depth of discharge, this represents a minimum capacity of around 18 kWh of electrical energy to survive the night. Assuming a specific energy density of 160 Wh/kg, this would mean a minimum mass of 114 kg for the batteries. Additional batteries are needed to power the remaining subsystems during the

night, leading to an estimated total battery mass of around 130 kg. This consequent weight could be significantly reduced in the future with promising technologies such as hybrid Li-metal batteries.

3.4 Communication And Data Handling System

According to the DRM, the airship will image the walls of the *Valles Marineris* using a hyperspectral camera. Hyperspectral images, though they can be compressed to an extent, produce very large volumes of data, which must somehow be communicated back to Earth. Transmittable data quantity will be the main driving consideration in the design of the communications system. As such, Direct-To-Earth and Direct-From-Earth communications are out of the question, as the data transmission speeds are too low (we can only hope for about 0.7 MB/sol)

The envisaged solution is the use of the Mars Relay Network (MRN) [21], which has been relaying communications between Earth and surface activities on the planet Mars for NASA and the ESA for about two decades now. It has allowed these space agencies' landers and rovers to communicate with Earth more quickly, reliably and efficiently, simplifying mission design and reducing mission costs. It is based on the Electra telecommunication and navigation package hardware [22], which is currently installed on 5 satellites orbiting Mars.

Nonetheless, even using the MRN, we can expect to return only at most (roughly) 900 MB/sol. However, when compared to the added cost and complexity of implementing a dedicated areostationary orbiting relay, this seems like a good trade-off.

The consequences of this choice are quite important though :

- The relatively small data volume which can be sent back might be quite problematic for the science experiment. One of the instruments currently envisaged for the payload is a hyperspectral camera, which produces 4 dimensional images. Despite the relatively high compression rates achievable nowadays (see [23]), these remain huge data volumes.

  A possibility would be to cache the full-sized images in an on-board memory until the flight phase of the mission is over, and only send highly compressed 'thumbnails' during the flight phase.

- The relatively long periods between satellite communications windows means that the airship must exhibit a high level of autonomy and decision ability. This will be addressed in the next sections (see subsubsection 3.5.2).

3.5 Navigation and Guidance

3.5.1 Simulated Airship Dynamics

3.5.1.1 Method

In order to understand the navigational limitations of the airship, the stability of the proposed airship shall be investigated a little closer using a simple dynamics simulation. The goal of the simulation is to get a rough idea of how the 'uncontrolled' system might behave. As such, the effects of the inner balloon are not taken into account in this model. Additionally, the gyroscopic effect of the spinning propellers has been neglected, as, by design, such moments shall internally cancel out in the propulsion system. The aerodynamic lift generated as the balloon travels against the wind is also neglected in this simulation.

3.5.1.2 Theory

The airship is assumed to be at equilibrium altitude: the buoyancy force B produced by the balloon will be assumed equal to the total weight W of the airship, which lets us solve for the initial altitude. The inner ballast balloon is assumed empty, and is therefore neglected in this simulation.

For simplicity, the propulsion engines are considered to be running at a constant power. The resulting thrust T is calculated according to Froude's Actuator Disc theory (see [24] and paragraph 3.2.4.1). The drag force F_{drag} acting on the balloon is calculated as proposed by the Scientific Ballooning Handbook [12].

Using these four forces and their average application points on the airship, the moments M acting on the airship can be estimated. We additionally add a term $Q_{drag}(\dot{\theta}, \ddot{\theta})$ to take into account the torque generated by drag on the surface of the balloon, as proposed in [25].

The dynamics of the airship's center of mass $(\ddot{x}, \ddot{\theta})$ are calculated using the added mass theory [26], where an additional 'virtual mass' m_a of air representing the aerodynamic boundary layer is considered. Since the airship is approximately spherical, the added inertia I_a is considered to be zero.

$$m_a = \frac{2}{3}\pi r_b^3 \rho_{atm} \quad (1)$$

$$\ddot{x} = \frac{W + B + T + F_{drag}}{m + m_a} \quad (2)$$

$$\ddot{\theta} = \frac{M_W + M_B + M_T + M_{drag} + Q_{drag}}{I + I_a} \quad (3)$$

3.5.1.3 Results and Discussion

The numerical simulation of the described system yielded the following results concerning the dynamic stability : In the worst case (Figure 12), when the airship is

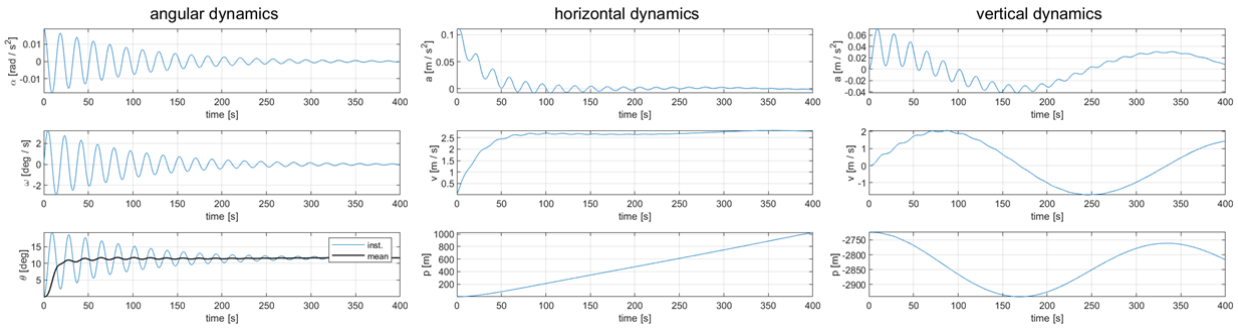

Figure 12: The simulated angular dynamics of the airship display relatively large oscillations which take a long time to decay.

fighting a head wind of 10 m/s, it was found that the system would oscillate with a period of roughly 17.3 s, with an initial amplitude of $\pm$ 6° about a mean of 10°. Due to the extremely low density of the martian atmosphere, the oscillations take a very long time to decay, only falling to about $\pm$ 0.6° after over 400 s.

Additionally, the simulation also revealed the 'minimum stopping distance' required by the airship. In other words: if the airship is drifting with the wind and suddenly powers up its propulsion, what is the time or distance required for it to come to a full standstill? Depending on the air density (which changes with altitude and season), a deceleration time ranging from 50 s to 100 s was found, which corresponded to a distance over land of 240 m to 320 m.

It is important to note that the obtained results are extremely dependent on the distribution of mass between gondola and balloon, and that small changes there can lead to large changes in the dynamic behavior of the airship, with oscillation periods ranging from 10 s to 20 s. A generous margin of safety shall therefore be taken on these results. The maximum swing amplitude of the airship shall be considered as 20°, and the maximum swing speed as 4°/s. The stopping distance d_{safety} will be considered as 700 m.

The effect of this oscillation on the on-board instrumentation is not negligible, and the design of any exteroceptive sensor used aboard will need to take it into account. The resolution of the information gathered by the sensors will be severely limited by motion blur, unless instrument stabilization is provided.

3.5.2 Navigation System

3.5.2.1 Obstacle Detection

The airship must detect potentially hazardous objects before it enters into an inevitable collision course with it. For this, radar ranging is considered: radar altimeters are used in commercial aviation to determine an aircraft's height above ground level, and radar ranging is used in autonomous vehicles to determine the distance to other vehicles on the road. Such radars are small, lightweight, not very powerful, and have a limited range (between 300 m and 760 m), and a limited spatial resolution, with typical beam widths ranging between 30°and 120°. They also have the advantage that several can be used at once without fear of interference, as they can use different frequencies or chirps. Thus a very rough directional proximity map of the close environment could be obtained with COTS technology.

3.5.2.2 Localisation & Mapping

Thanks to the developing autonomous vehicle industry, visual Simultaneous Localization And Mapping (SLAM) algorithms are quite well established for robotic applications, and could be very useful for 'global' navigation. However, due to the above-mentioned issue of motion-blur, it will be important to actively stabilize any on-board cameras. This stabilization will have to run at a relatively high frequency, and cover a fairly large angular range. For this, a 'tactical-grade' IMU will be necessary.

A well-integrated system will use both the data from the visual SLAM as well as from the IMU to achieve a good localisation in an poorly known environment. Maps created from HiRISE and MOLA data can be pre-loaded into memory and used as a starting point to simplify the SLAM localisation problem.

3.5.2.3 Path Planning

The global map generated by the SLAM algorithm must be used to generate a path for the airship to follow. The method considered for this is a multidimensional potential field. The trajectory is calculated from this potential field using gradient descent.

The potential field is a linear combination of :

- Repulsive obstacles, which are represented as locations of infinite 'potential energy', with an influence

trailing off to zero over the safety distance d_{safety}. Obstacles will therefore 'push' the airship away.

- An attractive goal, specified by mission operators on Earth, is the point of lowest potential. It is represented using either a quadratic or linearly growing potential to lead towards it.
- Small random shifts in order to avoid getting trapped in local minima (though proper weighting of the different fields will go a long way towards avoiding local minima in the first place).

The field can be augmented using more environmental fields, such as fields modeling the influence of wind and gravity. If an unattainable goal is given to the airship (e.g. it is within d_{safety} of an obstacle), it will be drawn to the closest 'safe' point to the goal.

3.5.2.4 Control

Once a trajectory has been established, it should be tracked by the airship's motion controller, which controls the propulsion system and the pumps to the inner ballast balloon. This will be a very complex piece of software, as it needs to take into account a number of different constraints due to the airship's hardware, as well as a constantly changing environment. To accomplish this, Model Predictive Control (MPC) is very attractive, as it permits the use of hard and soft constraints :

- Physical hard constraints, which can never be violated, such as available propulsion power, available inner balloon volume, airship dynamics
- Behavioral hard constraints, which should never be violated, such as terrain intersection or maximum / minimum balloon superpressure.
- Soft constraints, which can be violated only if there is no other solution. These include safety distance to obstacles, safety margins for balloon superpressure, inner balloon volume and propulsion power, top speed and maximum altitude
- The cost function, which covers the 'normal' optimization space containing trajectory tracking and station keeping, predicted gondola stability and energy efficiency

The trajectory tracking part of the cost function can directly use the potential field provided by the path planning submodule. This will result in a controller which acts as if a virtual 'force' were driving it towards the goal at all times. Using these techniques, the navigation system shall be sufficiently autonomous and robust to fulfill the airship's mission.

4 Conclusion

This continuation of the feasibility study on the Martian exploration airship did not find any insurmountable difficulties which would render the project impossible. We were also able to highlight the critical parameters which need to be refined in future work on the study.

4.1 Summary of Findings

We started by describing the airship and the design reference mission from a systems engineering perspective. For this, we presented a system breakdown structure and described the different subsystems involved. A corresponding mass budget was established, estimating a gross weight between 750 kg and 950 kg. In addition, we proposed a concept of operations describing the different flight phases from the Mars orbit insertion to the airship end-of-life.

The remaining sections were dedicated to the progress made on specific subsystems.

- *Envelope* : The pumpkin shape composite envelope as well as the inner balloon have been integrated as a subsystem of the airship system. The main design parameters have been identified and their impact on the mission have been discussed. The Mars Climate Database allowed us to estimate the main quantities such as hydrogen quantity and the mass of the envelope (including inner balloon). A simplified mechanical model was used to estimate the required thickness of the airship's envelope in order to withstand the stress due to thermal expansion of the lifting gas. Finally, the minimum required superpressure for the envelope to stay inflated was estimated at 1.2 times the surrounding atmospheric pressure.
- *Propulsion* : After having derived the requirements and constraints associated to Martian atmospheric flight, a preliminary design of propeller propulsion system was performed. A simple momentum balance highlighted the poor propeller efficiency to be expected, which will inevitably increase the required mass of batteries. Then, we used the blade element method to calculate the approximate propeller settings needed to achieve the propulsion requirements. It was concluded by a first proposition consisting of four sets of two-bladed contra-rotating propellers with 1.5 m diameter, driven by brushless DC motors. Horizontal control is applied via differential thrust. It shall be further investigated whether a vertical component control is needed in addition to the inner ballast balloon system.
- *Power* : A heavy power consumption can be expected from the propulsion system. Electrical power is

generated by solar cells implemented on top of the envelope. About 110 kg of batteries are needed to store enough power to compensate the absence of solar radiance during the night. About 260 m^2 of solar cells are necessary to reload the batteries during the day while also providing power to the other subsystems.

- *Communication and Data Handling* : Communicating with the airship on Mars would be possible via the existing Mars Relay Network. This has the advantage of allowing relatively decent transmission volumes, while keeping the mass and power consumption of the communications system quite low. The trade-off is the infrequent (and irregular) communications windows imposed by the orbits of the MRN.

- *Navigation and Guidance* : We described how the airship's autonomous navigation can be achieved through a combination of instruments : an IMU to provide high-speed movement updates; a stabilized vision system to feed a SLAM algorithm, allowing the airship to localize itself and create a detailed map of its surroundings; and finally a ranging radar, to confirm the depth estimations and avoid any potentially damaging contact with the landscape. The radar and IMU should also allow for night-time navigation, when the vision system will operate at a much reduced frame rate and resolution. They will also provide some robustness against atmospheric dust.

4.2 Further Work

The next step required to advance the study will be to continue feasibility studies on the other subsystems of the airship, to improve the accuracy of these mass and power budgets. It will be especially necessary to look into the deployment phase, which will determine a number of aspects related to the structure and CONOPS. Another extremely important aspect of the project which must be investigated in greater depth is the science mission: fixing the scientific objectives will help to shape the CONOPS, determine the specifications of the payload instrument(s) and set specific design goals for all other subsystems.

Acknowledgements

We would like to extend our gratitude to the people who allowed us to work on this fascinating study, and who supported us with their knowledge and advice : Mr. Pierre Brisson and Prof. Claude Nicollier of the Mars Society Switzerland for their feedback and insights; Ms. Alice Barthe and Ms. Laurène Delsupexhe of WoMars, for closely following the project and advising us on critical points; Mr. Roméo Tonasso for generously sharing his time, knowledge and resources. We would also like to thank Mr. Ehouarn Millour for graciously lending us access to the Mars Climate Database, without which none of this would have been possible.

References

[1] NASA. *Mars Helicopter*. URL: https://mars.nasa.gov/technology/helicopter/ (visited on 26/11/2021).

[2] V. V. Kerzhanovich et al. 'Mars Aerobot Validation Program'. In: AIAA Balloon Technology Conference 1999. American Institute of Aeronautics and Astronautics, 1999. URL: https://ntrs.nasa.gov/api/citations/20000058137/downloads/20000058137.pdf (visited on 24/04/2022).

[3] CNES. 'Des ballons pour la science'. In: *Cnes Magazine* n°11, Les ballons (2001), p. 13. URL: https://cnes.fr/sites/default/files/cnes-multimedia/data/cnes_fr/cnesmag/cnesmag11_FR_dossier.pdf (visited on 31/05/2022).

[4] Roméo Tonasso, Laurène Delsupexhe and Alice Barthe. 'Can An Airship Explore Mars?' In: *GLEX 2021*. Global Space Exploration Conference. 2021, p. 62378. URL: https://iafastro.directory/iac/paper/id/62378/abstract-pdf/GLEX-2021,3,1,8,x62378.brief.pdf?2021-03-04.10:06:29 (visited on 02/06/2022).

[5] I. Mitrofanov et al. 'The evidence for unusually high hydrogen abundances in the central part of Valles Marineris on Mars'. In: *Icarus* 374 (2022), p. 114805. ISSN: 0019-1035. DOI: https://doi.org/10.1016/j.icarus.2021.114805. URL: https://www.sciencedirect.com/science/article/pii/S0019103521004528 (visited on 02/06/2022).

[6] Diedrich T. F. Möhlmann et al. 'Fog phenomena on Mars'. In: *Planetary and Space Science* 57.14 (2009), pp. 1987–1992. ISSN: 0032-0633. DOI: https://doi.org/10.1016/j.pss.2009.08.003. URL: https://www.sciencedirect.com/science/article/pii/S0032063309002323 (visited on 02/06/2022).

[7] Cecilia W. S. Leung et al. 'Fogs and Clouds are a Potential Indicator of a Local Water Source in Valles Marineris'. In: *EGU General Assembly Conference Abstracts*. EGU General Assembly Conference Abstracts. Apr. 2016, EPSC2016-15346, EPSC2016–15346. URL: https://ui.adsabs.

harvard.edu/abs/2016EGUGA..1815346L (visited on 02/06/2022).

[8] David E. Stillman, Timothy I. Michaels and Robert E. Grimm. 'Characteristics of the numerous and widespread recurring slope lineae (RSL) in Valles Marineris, Mars'. In: *Icarus* 285 (Mar. 2017), pp. 195–210. DOI: 10.1016/j.icarus.2016.10.025. (Visited on 28/06/2022).

[9] Willi Schur. 'Analysis of load tape constrained pneumatic envelopes'. en. In: *40th Structures, Structural Dynamics, and Materials Conference and Exhibit*. St. Louis,MO,U.S.A.: American Institute of Aeronautics and Astronautics, Apr. 1999. DOI: 10.2514/6.1999-1526. URL: https://arc.aiaa.org/doi/10.2514/6.1999-1526 (visited on 06/12/2021).

[10] Ehouarn Millour et al. 'The Mars Climate Database (MCD version 5.3)'. In: *EGU General Assembly Conference Abstracts*. EGU General Assembly Conference Abstracts. Apr. 2017, p. 12247. URL: https://ui.adsabs.harvard.edu/abs/2017EGUGA..1912247M (visited on 31/05/2022).

[11] Anthony J. Colozza and Analex Corporation. 'Comparison of Mars Aircraft Propulsion Systems'. In: NASA/CR—2003-212350 (2003), p. 87.

[12] A. L. Morris. *Scientific Ballooning Handbook*. Boulder, Colorado: National Center For Atmospheric Research, 1975, p. 478.

[13] S. Maurice et al. 'In situ recording of Mars soundscape'. In: *Nature* 605.7911 (May 2022), pp. 653–658. ISSN: 1476-4687. DOI: 10.1038/s41586-022-04679-0. URL: https://doi.org/10.1038/s41586-022-04679-0 (visited on 06/06/2022).

[14] Justin Winslow et al. 'Basic Understanding of Airfoil Characteristics at Low Reynolds Numbers (104–105)'. In: *Journal of Aircraft* 55.3 (May 2018), pp. 1050–1061. ISSN: 0021-8669, 1533-3868. DOI: 10.2514/1.C034415. URL: https://arc.aiaa.org/doi/10.2514/1.C034415 (visited on 22/10/2021).

[15] Michael S. Selig. 'Low Reynolds Number Airfoil Design Lecture Notes'. In: (2003), p. 43.

[16] Michael S. Selig, ed. *Summary of low speed airfoil data*. Virginia Beach, Va: SoarTech Publications, 1995. 1 p. ISBN: 978-0-9646747-1-4.

[17] Witold J. F. Koning, Ethan A. Romander and Wayne Johnson. 'Performance Optimization of Plate Airfoils for Martian Rotor Applications Using a Genetic Algorithm'. In: *NASA Technical Reports* (2019), p. 16.

[18] Masayuki Anyoji et al. 'Effects of Mach Number and Specific Heat Ratio on Low-Reynolds-Number Airfoil Flows'. In: *AIAA Journal* 53.6 (June 2015), pp. 1640–1654. ISSN: 0001-1452, 1533-385X. DOI: 10.2514/1.J053468. URL: https://arc.aiaa.org/doi/10.2514/1.J053468 (visited on 14/12/2021).

[19] Auld and Srinivas. *Aerodynamics for Students*. URL: http://www.aerodynamics4students.com (visited on 15/12/2021).

[20] Mark Drela. 'XFOIL: An Analysis and Design System for Low Reynolds Number Airfoils'. In: *Low Reynolds Number Aerodynamics*. Ed. by Thomas J. Mueller. Red. by C. A. Brebbia et al. Vol. 54. Series Title: Lecture Notes in Engineering. Berlin, Heidelberg: Springer Berlin Heidelberg, 1989, pp. 1–12. ISBN: 978-3-642-84010-4. DOI: 10.1007/978-3-642-84010-4_1. URL: http://link.springer.com/10.1007/978-3-642-84010-4_1 (visited on 15/12/2021).

[21] NASA JPL. *Mars Relay Network*. URL: https://eyes.nasa.gov/apps/mrn (visited on 05/06/2022).

[22] L3Harris. *Mars UHF Transceiver*. Datasheet. 2020. URL: https://www.l3harris.com/sites/default/files/2020-07/ims_eo_datasheet_UHF_Mars_Transmitter.pdf (visited on 02/06/2022).

[23] Yubal Barrios et al. 'SHyLoC 2.0: A Versatile Hardware Solution for On-Board Data and Hyperspectral Image Compression on Future Space Missions'. In: *IEEE Access* 8 (2020), pp. 54269–54287. DOI: 10.1109/ACCESS.2020.2980767. URL: https://accedacris.ulpgc.es/bitstream/10553/71251/1/ShyLOC2.pdf (visited on 03/06/2022).

[24] Z. S. Spakovszky. *16.Unified: Thermodynamics and Propulsion*. 2007. Chap. 11.7 Performance of Propellers. URL: https://web.mit.edu/16.unified/www/FALL/thermodynamics/notes/node86.html (visited on 31/05/2022).

[25] U. Lei, C. Y. Yang and K. C. Wu. 'Viscous torque on a sphere under arbitrary rotation'. In: *Applied Physics Letters* 89.18 (2006), p. 181908. DOI: 10.1063/1.2372704. eprint: https://doi.org/10.1063/1.2372704. URL: https://doi.org/10.1063/1.2372704 (visited on 31/05/2022).

[26] G. G. Stokes. 'On the Effect of the Internal Friction of Fluids on the Motion of Pendulums'. In: *Transactions of the Cambridge Philosophical Society* 9 (Jan. 1851), p. 8. URL: https://ui.adsabs.harvard.edu/abs/1851TCaPS...9....8S (visited on 31/05/2022).